BIOCHEMISTRY
including biophysical chemistry & molecular biology

Article

pubs.acs.org/biochemistry

Substrate Specificity, Substrate Channeling, and Allostery in BphJ: An Acylating Aldehyde Dehydrogenase Associated with the Pyruvate Aldolase BphI

Perrin Baker, Jason Carere, and Stephen Y. K. Seah*

Department of Molecular and Cellular Biology, University of Guelph, Guelph, Ontario, Canada

Supporting Information

ABSTRACT: BphJ, a nonphosphorylating acylating aldehyde dehydrogenase, catalyzes the conversion of aldehydes to form acyl-coenzyme A in the presence of NAD^+ and coenzyme A (CoA). The enzyme is structurally related to the nonacylating aldehyde dehydrogenases, aspartate-β-semialdehyde dehydrogenase and phosphorylating glyceraldehyde-3-phosphate dehydrogenase. Cys-131 was identified as the catalytic thiol in BphJ, and pH profiles together with site-specific mutagenesis data demonstrated that the catalytic thiol is not activated by an aspartate residue, as previously proposed. In contrast to the wild-type enzyme that had similar specificities for two- or three-carbon aldehydes, an I195A variant was observed to have a 20-fold higher catalytic efficiency for butyraldehyde and pentaldehyde compared to the catalytic efficiency of the wild type toward its natural substrate, acetaldehyde. BphJ forms a heterotetrameric complex with the class II aldolase BphI that channels aldehydes produced in the aldol cleavage reaction to the dehydrogenase via a molecular tunnel. Replacement of Ile-171 and Ile-195 with bulkier amino acid residues resulted in no more than a 35% reduction in acetaldehyde channeling efficiency, showing that these residues are not critical in gating the exit of the channel. Likewise, the replacement of Asn-170 in BphJ with alanine and aspartate did not substantially alter aldehyde channeling efficiencies. Levels of activation of BphI by BphJ N170A, N170D, and I171A were reduced by ≥3-fold in the presence of NADH and ≥4.5-fold when BphJ was undergoing turnover, indicating that allosteric activation of the aldolase has been compromised in these variants. The results demonstrate that the dehydrogenase coordinates the catalytic activity of BphI through allostery rather than through aldehyde channeling.

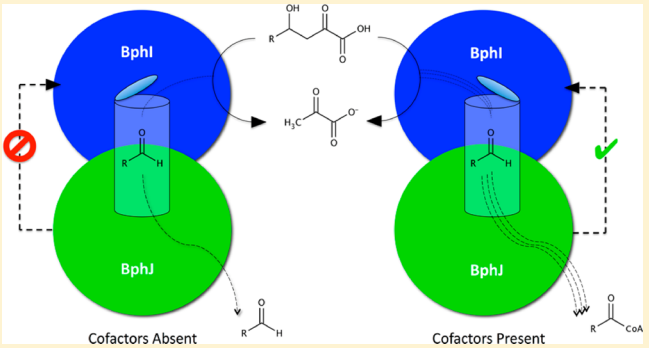

Aldehyde dehydrogenases (ALDHs) are evolutionarily diverse enzymes present in both prokaryotic and eukaryotic organisms that are involved in numerous biological functions, including central metabolism, osmotic protection, cellular differentiation, and detoxification pathways. They can be classified as phosphorylating or nonphosphorylating ALDHs, producing activated or nonactivated acid products. Both groups of ALDHs share a common acylation step, whereby the thiolate of cysteine acts as a nucleophile to attack the carbonyl carbon of the aldehyde forming a thiohemiacetal intermediate. Following the transfer of a hydride to NAD^+, a thioacylenzyme intermediate is produced. The deacylation step, however, differs depending on the nature of the acyl acceptor.[1−3] In phosphorylating dehydrogenases, inorganic phosphate acts as the acyl acceptor, while in nonphosphorylating dehydrogenases, the thioacylenzyme intermediate undergoes nucleophilic attack by either water (CoA-independent/hydrolytic) or coenzyme A (CoA-dependent/acylating), leading to the formation of either nonactivated or CoA-activated acids, respectively. Hydrolytic ALDHs undergo a sequential kinetic mechanism with NAD(P)H dissociating last,[4−7] whereas CoA-dependent ALDHs exhibit a ping-pong mechanism whereby the release of the reduced nicotinamide cofactor occurs before the binding of coenzyme A and the transthioesterification step.[8−10] While mechanistic and structural aspects of hydrolytic ALDHs have been extensively studied,[11−17] considerably less is known about CoA-dependent ALDHs.[18]

BphJ is a nonphosphorylating CoA-dependent ALDH from the polychlorinated biphenyl (PCB) pollutant-degrading bacterium *Burkholderia xenovorans* LB400 (Scheme 1).[19,20] BphJ forms a stable complex with the aldolase, BphI, which catalyzes the aldol cleavage of 4-hydroxy-2-oxoacids to pyruvate and an aldehyde.[21,22] Aldehyde intermediates, up to six carbons in length, can be channeled directly from the active site of BphI to BphJ, via a molecular tunnel, with an efficiency of >80%.[19] Because aldehydes are reactive, substrate channeling sequesters the aldehydes from cellular components and overcomes the inefficiency of the dehydrogenase, BphJ, for processing exogenous aldehydes because of high K_m values.[20] When

Received: March 30, 2012
Revised: May 8, 2012
Published: May 10, 2012

   dx.doi.org/10.1021/bi300407y | *Biochemistry* 2012, 51, 4558−4567

Scheme 1. Reaction Catalyzed by BphJ[a]

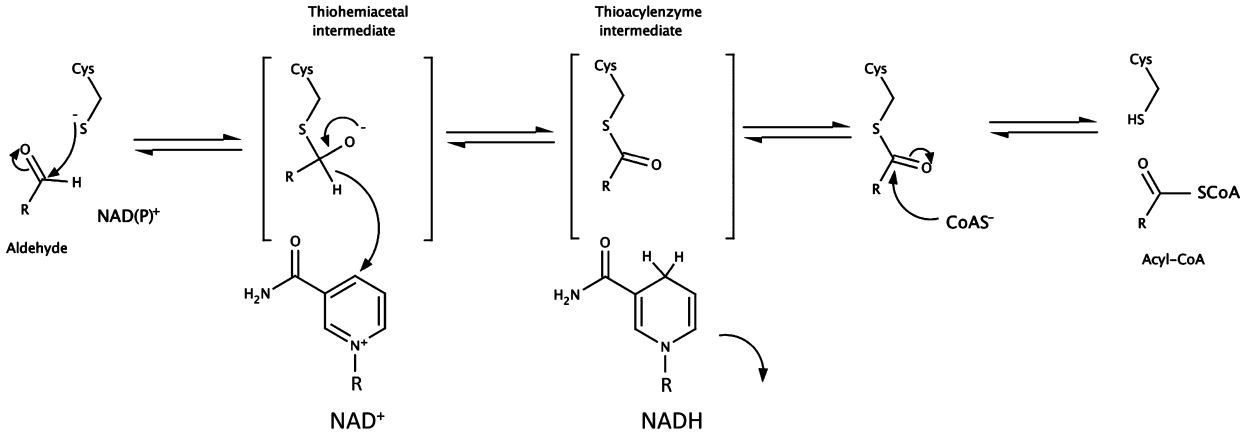

[a]Nucleophilic attack by cysteine on the aldehyde results in the formation of a thiohemiacetal intermediate. Hydride transfer reduces the NAD^+ cofactor to NADH and leads to the formation of a thioacylenzyme intermediate. NADH leaves the active site, and the deacylation step occurs by the nucleophilic attack of coenzyme A on the thioacylenzyme intermediate, leading to the formation and release of acyl-CoA product.

bound to BphJ, the nicotinamide cofactor increases the aldol cleavage activity of BphI by ~5-fold.[19,20]

The crystal structure of DmpG-DmpF [Protein Data Bank (PDB) entry 1NVM], an ortholog of BphI-BphJ from the phenol degradation pathway of *Pseudomonas putida* CF600, is available.[23] Interestingly, DmpF is not structurally related to methylmalonate-semialdehyde dehydrogenase (PDB entry 1T90) from *Bacillus subtilis*, which is the only other acylating aldehyde dehydrogenase with a known structure.[24] Instead, it was reported to structurally resemble glyceraldehyde-3-phosphate dehydrogenase, a phosphorylating hydrolytic dehydrogenase.[23] It was further demonstrated through hydrogen−deuterium exchange mass spectrometry experiments that NAD^+ and coenzyme A share the same binding site.[25] While other enzymes, such as succinic synthetases, utilize the Rossmann folds to bind coenzyme A,[26−28] DmpF and related enzymes appear to be unique in that they utilize this domain to bind both the nicotinamide cofactor and coenzyme A. Conversely, it has been suggested that NAD^+ and CoA in the unrelated acylating ALDH, methylmalonate semialdehyde dehydrogenase, bind to separate domains of the enzyme.[18]

Here active site residues in BphJ were replaced by site-specific mutagenesis. The catalytic thiol and residues important for substrate specificity, coenzyme binding, and allosteric regulation were identified. Our results shed light on the molecular basis for the divergence of function in related ALDHs.

EXPERIMENTAL PROCEDURES

Chemicals. All aldehydes, NAD^+, NADH, L-lactate dehydrogenase (LDH, rabbit muscle), all aldehydes, and alcohol dehydrogenase (*Saccharomyces cerevisiae*) were from Sigma-Aldrich (Oakville, ON). Ni-NTA Superflow resin was obtained from Qiagen (Mississauga, ON). 4(*S*)-Hydroxy-2-oxopentanoate was synthesized using BphI according to previously described methods.[21] Aldehyde dehydrogenase from *S. cerevisiae* was obtained from Calzyme (San Luis Obispo, CA). All other chemicals were analytical grade and were obtained from Sigma-Aldrich or Fisher Scientific (Nepean, ON).

DNA Manipulation. DNA was purified, digested, and ligated using standard protocols. *bphJ* was previously cloned into plasmid pET28a, and *bphI* was cloned into pBTL4-T7.[20] Site-directed mutagenesis was completed according to a modified Quikchange (Stratagene) method that uses non-overlapping primers (Table S1 of the Supporting Information).[29] DNA of putative mutants was sequenced at the Guelph Molecular Supercenter to confirm the presence of desired mutations and the absence of secondary mutations.

Protein Expression and Purification. Expression and purification of BphI-BphJ was completed as previously described.[20] Sodium dodecyl sulfate−polyacrylamide gel electrophoresis was performed, and gels were stained with Coomassie Blue to assess purity. The purified enzyme was aliquoted and stored in 20 mM HEPES buffer (pH 8.5) with 10 mM DTT at −80 °C. The concentration of enzyme was determined using the Bradford method.[30]

Dehydrogenase Activity Assays. The substrate specificity of the dehydrogenase was determined using 0.4 mM NAD^+ and 0.1 mM coenzyme A unless stated otherwise, and aldehyde concentrations were varied from at least $0.1K_m$ to $5K_m$. Concentrations of aldehyde stocks were determined by measuring the stoichiometric oxidation of NADH using alcohol dehydrogenase. Cofactor specificities were determined under similar conditions in which the acetaldehyde concentrations were held at 100 mM and concentrations of NAD^+ and CoA were varied between $0.1K_m$ and $5K_m$.

The effects of pH on k_{cat} and k_{cat}/K_m were studied in the pH range of 6.0−9.0 using a constant-ionic strength buffer containing 0.1 M Tris, 0.05 M acetic acid, and 0.05 M MES. All other conditions were the same as those of standard enzyme assays with the substrate acetaldehyde concentration varied from at least $0.1K_m$ to $5K_m$. Data were plotted using eq 1 by nonlinear regression in Leonora[31]

$$v = \frac{C}{1 + H/K_{a1}} \quad (1)$$

where C is the pH-independent value of k_{cat} or k_{cat}/K_m, H is the proton concentration, and K_{a1} is the ionization constant of groups involved in the reaction.

Aldolase Activity Assays. The aldolase cleavage activity was determined continuously or discontinuously by coupling the production of pyruvate to LDH and monitoring the oxidation of NADH.[20] All assays were performed in at least

dx.doi.org/10.1021/bi300407y | *Biochemistry* 2012, 51, 4558−4567

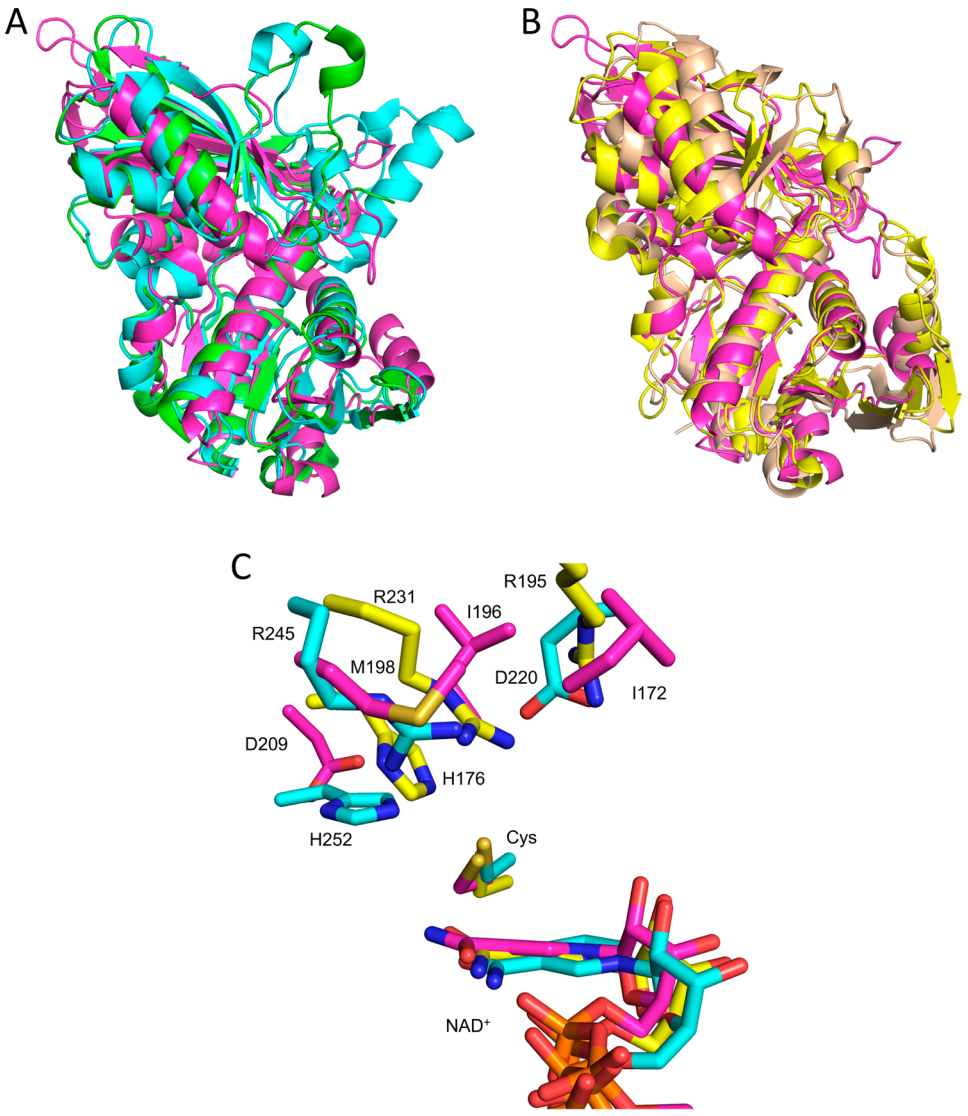

Figure 1. Superimposition of the nonphosphorylating acylating aldehyde dehydrogenase DmpF with structurally similar aldehyde dehydrogenases glyceraldehyde-3-phosphate dehydrogenase and aspartate-semialdehyde dehydrogenase. (A) Superimposition of the structure of DmpF with ASADHs (rmsd of 2.5−2.7 Å). (B) Superimposition of the structure of DmpF with GAPDHs (rmsd of 2.4−2.7 Å). DmpF from *P. putida* CF600 (PDB entry 1NVM) is colored pink. ASADH from *Vibrio colerae* (PDB entry 2R00) is colored green. ASADH from *Streptococcus pneumoniae* (PDB entry 2GZ3) is colored teal. Phosphorylating GAPDH from *Bacillus stearothermophilius* (PDB entry 3CMC) is colored yellow. GAPDH from *Arabidopsis thaliana* (PDB entry 3K2B) is colored tan. (C) Active site residues are not conserved with the exception of the putative catalytic cysteines. All residues in the active site of DmpF are conserved in BphJ with the exception of Met-198 that is replaced with Leu-197. DmpF from *P. putida* CF600 has carbon atoms colored magenta, GAPDH from *B. stearothermophilus* carbon atoms colored yellow, and ASADH from *S. pneumoniae* carbon atoms colored cyan. Oxygen and nitrogen atoms are colored red and blue, respectively.

duplicate, at 25 °C in a total volume of 1 mL using a Varian Cary 3 spectrophotometer with a thermojacketed cuvette holder. Standard continuous assays contained 0.4 mM NADH, 1 mM $MnCl_2$, and 19.2 units of LDH in 100 mM HEPES buffer (pH 8.0). The concentration of 4(*S*)-hydroxy-2-oxopentanoate (HOPA) was varied from 0.1K_m to 10K_m. Oxidation of NADH was monitored continuously at 340 nm with an extinction coefficient of 6200 M^{-1} cm^{-1}. To assess the activity of BphI in the absence of NADH, a discontinuous assay was utilized. Assay mixtures contain 1 mM $MnCl_2$, HOPA concentrations that varied from 0.1K_m to 10K_m, and 20 μg (80 μg for N170A and N170D) of BphI-BphJ in 100 mM HEPES buffer (pH 8.0). After 10 min, the reaction was quenched with 20 mM EDTA (pH 8.5) and 0.4 mM NADH. The amount of pyruvate produced was measured by an end point assay using LDH.

Test of Substrate Channeling. The amount of aldehyde channeled directly from the aldolase to the dehydrogenase without export to the bulk solvent was assessed using an enzyme competition assay previously described.[19] Unless otherwise stated, assays contained NAD^+ at a concentration of at least 5K_m, coenzyme A at a concentration of least 3K_m, 1 mM $MnCl_2$, and 5 μg of BphI-BphJ with 20 units of aldehyde dehydrogenase (ALDH), which converts aldehydes to acids and reduces NAD^+ to NADH. Reactions were quenched after 5 min with 24 μL of 3 N HCl and mixtures centrifuged for 3 min at 21000*g* to pellet the denatured enzyme. A 500 μL aliquot of the reaction mixture was subjected to high-performance liquid chromatography (HPLC) using an ÄKTA Explorer 100 (Amersham Pharmacia Biotech, Baie d'Urfe, QC) equipped with a HyPURITY C18 column (Thermo Scientific). The

dx.doi.org/10.1021/bi300407y | *Biochemistry* 2012, 51, 4558−4567

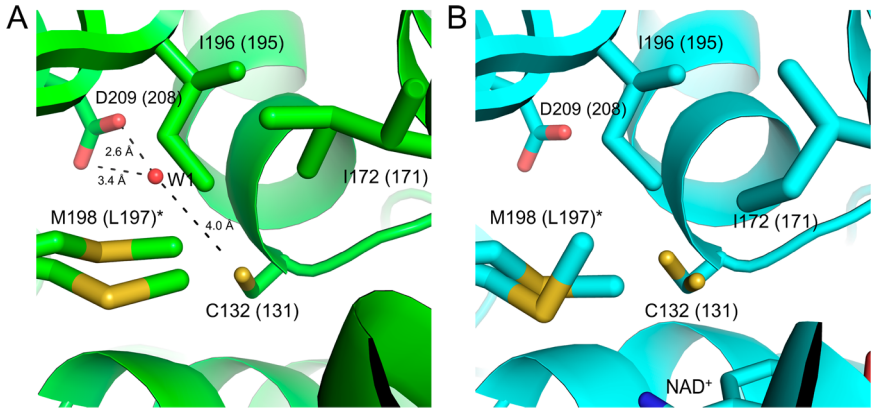

Figure 2. Active site of DmpF showing differences in the apo and NAD$^+$-bound structures. (A) Apo form of DmpF with the proposed catalytic thiol (Cys-132) oriented toward Asp-209 through hydrogen bonding with a bridging water molecule 4.0 Å from Cys-132 and 2.6 and 3.4 Å from Asp-209. (B) Holo form of DmpF depicting Cys-132 in a second conformation oriented toward the nicotinamide moiety of NAD$^+$, which is in turn hydrogen bonding to Asn-171. In this conformation, both Ile-172 and Met-198 change their rotameric configuration in comparison to the apoenzyme structure. Numbers in parentheses correspond to the residue numbers of BphJ. All residues are conserved with the exception of Met-198 that is replaced with Leu-197 in BphJ.

sample was eluted with a 50 mM sodium phosphate (pH 5.3)/acetonitrile mixture (47:3). The channeling efficiency was calculated by comparing the concentration of acetyl-CoA produced (determined using HPLC) to the concentration of 4-hydroxy-2-oxopentanoate utilized by BphI based on the amount of NADH produced by BphJ and ALDH (eq 2).[19]

$$\text{channeling efficiency (\%)} = \frac{[\text{acyl-CoA produced}]}{[\text{4-hydroxy-2-oxoacid utilized}]} \times 100\% \quad (2)$$

Dissociation Constant of NAD$^+$. The dissociation constant of NAD$^+$ was assessed by tryptophan fluorescence quenching upon NAD$^+$ binding. Experiments were completed using a PTI QuantaMaster C-61 steady-state fluorimeter (Photon Technology International, London, ON), with a 1 nm bandwidth for excitation (λ_{ex} = 290 nm) and a 2 mm bandwidth for emission (λ_{em} = 330 nm). Titrations were completed in 500 μL of 20 mM HEPES (pH 8.5) at 25 °C with 100 μg of enzyme. NAD$^+$ was added stepwise to the enzyme mixture. The fluorescence intensity was corrected for dilution factors, and the dissociation constant was calculated by fitting to eq 3, which describes binding to one site:

$$\frac{\Delta F}{F_o} \times 100 = \frac{\left(\frac{\Delta F_{max}}{F_o} \times 100\right) \times [S]}{K_d + [S]} \quad (3)$$

where $\Delta F/F_o \times 100$ is the percent fluorescence quenching (percent change in fluorescence relative to the initial value, F_o) following addition of a substrate at concentration [S]. Fitting was conducted using nonlinear regression using SigmaPlot 11.0.

RESULTS

Structural Analysis of the Dehydrogenase. The crystal structure of DmpF, an ortholog of BphJ, is composed of two domains, an N-terminal Rossmann fold spanning residues 6–119 and a C-terminal dimerization domain composed of residues 127–273 that is responsible for interacting with the aldolase.[32] Analysis using the DALI server[33] indicated that DmpF structurally resembles aspartate-β-semialdehyde dehydrogenase (PDB entry 2R00)[34] and glyceraldehyde-3-phosphate dehydrogenase (PDB entry 1CF2)[35] (Figure 1A,B), with root-mean-square deviations (rmsds) of 2.4 and 2.5 Å, respectively. Superimposition of these structures revealed that catalytic cysteines of these enzymes are equivalent in position to Cys-132 in DmpF. None of the other active site residues are conserved among the three enzymes (Figure 1C).

Significant movement in the Rossmann fold occurs between the apo and NAD$^+$-bound forms of DmpF, with an average rmsd of 1.8 Å. The active site, located between the NAD$^+$-binding domain and the dimzerization domain, contains the putative catalytic thiol, Cys-132 (Cys-131 in BphJ), on the N-terminal end of α_6.[25] This cysteine residue adopts two rotameric configurations in the DmpG-DmpF crystal structure (Figure 2). In the apo form, the thiol orients toward Asp-209 with a bridging water molecule 4.0 Å from the sulfur atom of Cys-132 and 2.6 and 3.4 Å from the carboxylic oxygens of Asp-209. In the NAD$^+$-bound form, the thiol is perpendicular to the nicotinamide moiety of NAD$^+$. It was previously proposed that changes in the conformation of Cys-132 and the bridging water are required to activate the thiol for nucleophilic attack on the carbonyl carbon of the aldehyde substrate.[23,36]

Three hydrophobic residues, Ile-172, Ile-196, and Met-198 (Ile-171, Ile-195, and Leu-197, respectively, in BphJ), form part of the interface between DmpF and the aldolase DmpG and also form the exit of the aldehyde channel connecting the two enzymes.[19,23] These residues have been proposed to act as a gate to control the passage of aldehydes that are channeled from the aldolase to the dehydrogenase.[23,36] This is partly supported by alteration of the rotameric configuration of Ile-172 and Ile-196 between the NAD$^+$-bound and NAD$^+$-free structures mediated by Asn-171 (Asn-170 in BphJ) in DmpF. Asn-171 undergoes a 166° rotation in the presence of NAD$^+$ relative to the apo structure, allowing the carboxamide of Asn-171 to form hydrogen bonds with the ribosyl hydroxyls of NAD$^+$. This movement results in changes to the Cα backbone, which subsequently affects the rotameric configuration of Ile-172 and Ile-196 (Figure 3A). In the apo form, Ile-172 is seen in multiple conformations, one of which is more predominant as visualized in the electron density, obtained from the Electron Density Server (Figure 3B).[37] The distance between the Cδ atom of Ile-172 and the Cγ_2 atom of Ile-196 in the apo structure (observed in two conformations) ranges from 3.4 to 3.7 Å. In the NAD$^+$-bound form, the distance between these

dx.doi.org/10.1021/bi300407y | Biochemistry 2012, 51, 4558–4567

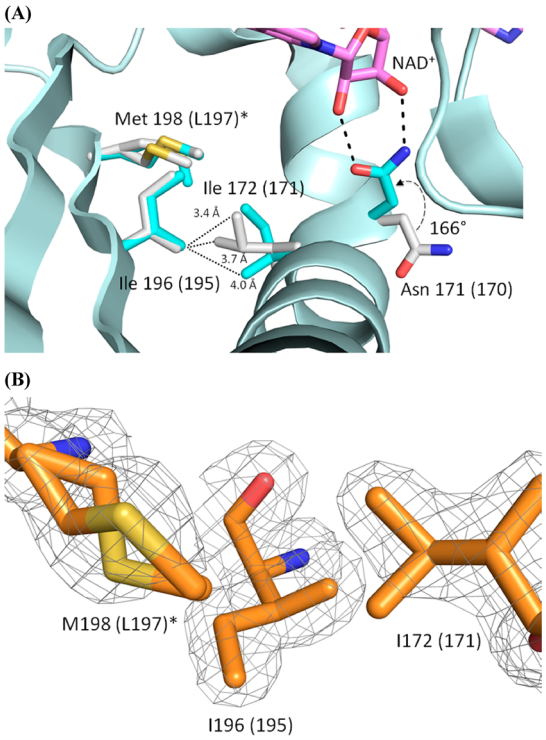

Figure 3. Structural changes upon NAD^+ binding in DmpF (A) Interaction of NAD^+ with Asn-171 of DmpF. In the presence of NAD^+, Asn-171 rotates 166° and forms hydrogen bonds with the hydroxyls of the nicotinamide ribose ring. This causes movement of the adjacent isoleucine (Ile-172), one of three residues that line the exit of the aldehyde channel leading to the dehydrogenase active site. Carbon atoms in the apo structure are colored gray, and the NAD^+-bound structure is depicted as a cartoon with blue carbon atoms. (B) Electron density of residues in the apo structure showing multiple conformations of Ile-172 and Met-198.

residues increases to 4.0 Å. It was therefore suggested on the basis of the crystal structure that Ile-172, Ile-196, and Met-198 in DmpF may gate the exit of channeled aldehydes from the aldolase and the opening of the gate is mediated via Asn-171 upon NAD^+ binding.[23]

To elucidate the function of these conserved residues in BphJ, we replaced Ile-171 with alanine and phenylalanine (I171A and I171F, respectively) and Ile-195 with the smaller alanine (I195A) as well as the bulker phenylalanine and tryptophan (I195F and I195W, respectively) residues. Asn-170 was replaced with alanine and aspartate (N170A and N170D, respectively). Finally, to identify the catalytic thiol and the role of Asp-208, we replaced Cys-131 with alanine and serine (C131A and C131S, respectively) and Asp-208 with alanine (D208A). All variants were expressed and purified in *E. coli* BL21(λDE3) to homogeneity using the same protocol developed for the wild-type enzyme.[20]

Analysis of Cys-131 and Asp-208. When Cys-131 was replaced with alanine (C131A) or serine (C131S), no detectable activity was observed (Table 1). Examination of these cysteine variants (C131A and C131S) by circular dichroism did not reveal significant differences in spectra relative to that of the wild-type (WT) enzyme (Figure S1 of the Supporting Information), suggesting that abrogation of catalysis is not the result of drastic changes in the structure of the enzyme. NAD^+ was still able to bind to the enzyme; however, the K_d was increased 20-fold compared to that of the wild-type

Table 1. Steady-State Kinetic Parameters of BphJ with Acetaldehyde as the Substrate[a]

enzyme	K_m (mM)	k_{cat} (s^{-1})	$k_{cat}/K_{m,app}$ (M^{-1} s^{-1})
WT	23.6 ± 1.8	17.2 ± 0.5	730 ± 60
C131A	NA	NA	NA
C131S	NA	NA	NA
D208A	18.7 ± 1.4	7.6 ± 0.2	406 ± 34

[a]Assays were performed at 25 °C and contained 0.4 mM NAD^+ and 0.1 mM coenzyme A in 100 mM HEPES buffer (pH 8.0) in a total volume of 1 mL. NA means not available.

enzyme. The aldolase, BphI, could form a stable complex with the cysteine variants of BphJ, and the associating aldolase had kinetic parameters similar to those of wild-type BphI, further supporting the premise that the aldolase–dehydrogenase complex is properly folded (Table S2 of the Supporting Information).

The pH dependence of the BphJ-catalyzed conversion of acetaldehyde to acetyl-CoA was determined over a pH range of 6.0–9.0 and was fit to a one-pK_a model with pK_a values of 8.49 ± 0.05 and 8.05 ± 0.03 for the free enzyme and enzyme–substrate complex, respectively (Figure 4). It was previously proposed that the putative catalytic thiol Cys-132 is activated via base attack from the bound water, which is activated by Asp-209 in DmpF.[23,36] Substitution of the equivalent Asp-208 in BphJ with alanine (D208A) resulted in a <2-fold difference in the steady-state catalytic efficiency (k_{cat}/K_m) for the dehydrogenase reaction relative to that of the wild-type enzyme. In addition, the pH dependency of the reaction was not significantly altered relative to that of the wild-type enzyme (pK_a values of 8.57 ± 0.08 and 8.08 ± 0.03 for the free enzyme and enzyme–substrate complex, respectively) (Figure 4). This suggests that Asp-209 is not involved in thiol activation.

Dehydrogenase Substrate Specificity. The wild-type enzyme exhibited similar catalytic efficiencies (k_{cat}/K_m) for acetaldehyde and propionaldehyde with a ∼2-fold lower catalytic efficiency for butyraldehyde compared to those for the smaller aldehydes (Table 2). Specificity for pentaldehyde was 10-fold lower than that for acetaldehyde primarily because of the high apparent K_m value for this substrate.

Both I171A and I171F exhibited preferences for aldehydes similar to that of the wild type (Table 2). In contrast, the I195A variant exhibited a 5-fold reduction in the specificity constant for acetaldehyde, because of the increase in the apparent K_m value. The specificity constants for butyraldehyde and pentaldehyde in this variant increased by approximately 9- and 20-fold, respectively, compared to that of the wild-type enzyme. The increase in specificity constants for longer chain aldehydes primarily resulted from lower K_m values (<10 mM for butyraldehyde and pentaldehyde). Significantly, the k_{cat}/K_m of the I195A variant for pentaldehyde is 20-fold higher than that of the wild-type enzyme, making it a more efficient enzyme for utilization of this longer chain aldehyde (1584 ± 156 M^{-1} s^{-1}) compared to the wild-type enzyme for its natural substrate, acetaldehyde (730 ± 60 M^{-1} s^{-1}). When Ile-195 was replaced with a phenylalanine or tryptophan, k_{cat}/K_m values were 5–20-fold lower than that of the wild type for aldehydes two to four carbons in length. An increase in the K_m for butyraldehyde in both I195F and I195W variants is responsible for the reduction in k_{cat}/K_m. Together, these results suggest that the alkyl chain of the aldehyde orients toward Ile-195 and that this residue is responsible for governing aldehyde substrate chain length

dx.doi.org/10.1021/bi300407y | *Biochemistry* 2012, 51, 4558–4567

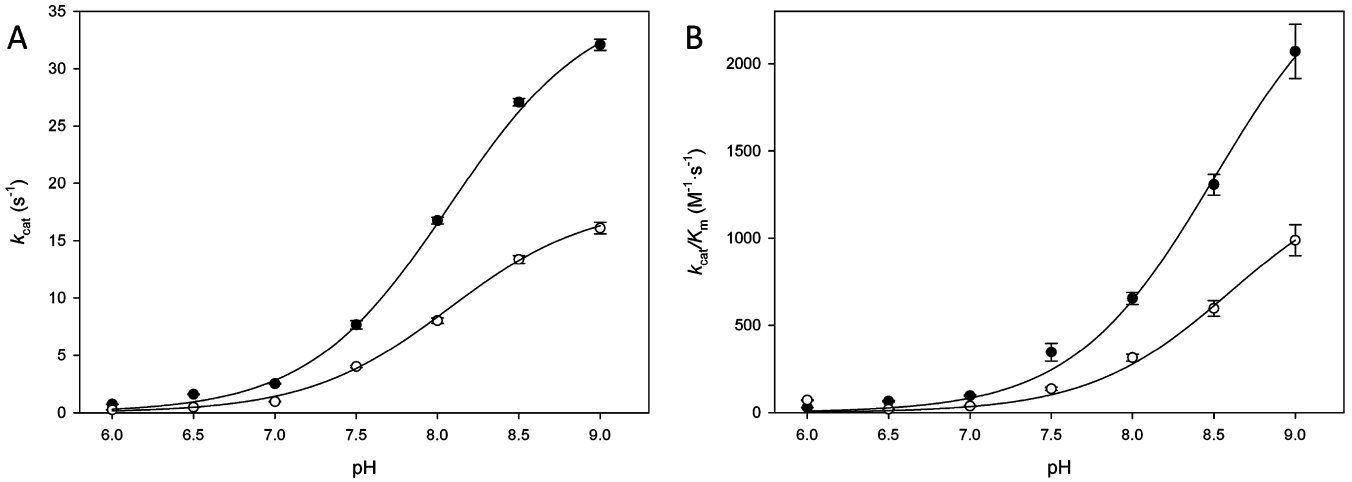

Figure 4. pH dependence of k_{cat} and k_{cat}/K_m for WT BphJ and the D208A variant. Assays were conducted in a constant-ionic strength buffer containing 0.1 M Tris, 0.05 M acetic acid, 0.05 M MES, and 1 mM $MnCl_2$. (A) pH dependence of k_{cat} of WT BphJ and the D208A variant (B) pH dependence of k_{cat}/K_m of WT BphJ and the D208A variant. WT (●) and D208A (○) for both panels.

Table 2. Substrate Specificity of BphJ in the Dehydrogenase Reaction[a]

enzyme	kinetic parameter	acetaldehyde (two carbons)	propionaldehyde (three carbons)	butyraldehyde (four carbons)	pentaldehyde (five carbons)	picolinaldehyde
WT	$K_{m,app}$ (mM)	23.6 ± 1.8	23.1 ± 1.7	31.7 ± 2.2	–	18.2 ± 1.3
	$k_{cat,app}$ (s^{-1})	17.2 ± 0.5	16.3 ± 0.5	9.5 ± 0.2	–	2.8 ± 0.1
	$k_{cat}/K_{m,app}$ (M^{-1} s^{-1})	730 ± 60	700 ± 50	300 ± 20	76 ± 3.1[b]	154 ± 12
I171A	$K_{m,app}$ (mM)	17.0 ± 1.4	20.4 ± 2.1	12.6 ± 1.2	–	3.2 ± 0.3
	$k_{cat,app}$ (s^{-1})	37.9 ± 1.2	24.9 ± 1.2	16.7 ± 0.9	–	1.9 ± 0.1
	$k_{cat}/K_{m,app}$ (M^{-1} s^{-1})	2224 ± 203	1219 ± 141	1323 ± 147	72.8 ± 4.9[b]	597 ± 53
I171F	$K_{m,app}$ (mM)	34.9 ± 3.5	27.2 ± 2.4	19.3 ± 1.3	–	12.0 ± 1.0
	$k_{cat,app}$ (s^{-1})	7.8 ± 0.3	6.0 ± 0.2	7.1 ± 0.2	–	2.4 ± 0.1
	$k_{cat}/K_{m,app}$ (M^{-1} s^{-1})	223 ± 23	221 ± 21	370 ± 29	38.7 ± 1.3[b]	202 ± 17
I195A	$K_{m,app}$ (mM)	133 ± 12	31.5 ± 2.7	4.6 ± 0.3	8.2 ± 0.8	6.9 ± 0.5
	$k_{cat,app}$ (s^{-1})	19.7 ± 0.9	12.1 ± 0.6	12.6 ± 0.3	13.0 ± 0.4	3.2 ± 0.1
	$k_{cat}/K_{m,app}$ (M^{-1} s^{-1})	147 ± 15	384 ± 35	2763 ± 181	1584 ± 156	468 ± 34
	$K_{m,app}$ (mM)	33.7 ± 3.2	45.7 ± 4.1	–	–	–
I195F	$k_{cat,app}$ (s^{-1})	15.4 ± 0.6	7.6 ± 0.3	–	–	–
	$k_{cat}/K_{m,app}$ (M^{-1} s^{-1})	457 ± 48	167 ± 16	43.3 ± 2.3[b]	34.6 ± 2.3[b]	0.76 ± 0.03[b]
	$K_{m,app}$ (mM)	45.6 ± 4.0	79.5 ± 6.9	–	–	–
I195W	$k_{cat,app}$ (s^{-1})	6.9 ± 0.3	3.4 ± 0.2	–	–	–
	$k_{cat}/K_{m,app}$ (M^{-1} s^{-1})	152 ± 14	42.5 ± 4.1	45.8 ± 1.4[b]	26.5 ± 1.1[b]	0.11 ± 0.01[b]

[a]Assays were performed at 25 °C and contained 5 μg of BphJ variants, 1 mM $MnCl_2$, 100 μM CoA, and 400 μM NAD^+ with varying concentrations of aldehydes in 100 mM HEPES buffer (pH 8.0). Assays were performed at 25 °C and contained 5 μg of BphJ variants, 1 mM $MnCl_2$, 200 μM CoA, and 800 μM NAD^+ with concentrations of picolinaldehyde varying between 0.1K_m and at least 5K_m in 100 mM HEPES buffer (pH 8.0). [b]Because of the low substrate solubility or high apparent K_m for the substrate, the specificity constant can be estimated from the linear gradient of specific activity vs substrate concentration.

specificity. The apparent K_m values of NAD^+ in I171F and I195 variants were not significantly perturbed (≤3-fold) relative to that of the wild-type enzyme.

The k_{cat} for picolinaldehyde in wild-type BphJ was approximately 5-fold lower compared to that for the natural substrate, acetaldehyde. The I171A and I195A variants exhibited the highest catalytic efficiencies for picolinaldehyde, while the incorporation of an aromatic residue at position 195 (I195F and I195W) resulted in >200-fold reductions in k_{cat}/K_m, possibly because of steric hindrance with the large picolinaldehyde side chain (Table 2).

Cofactor Binding and Specificity. BphJ was tested for its ability to use various thiols during the deacylation step of the reaction. The enzyme could utilize dithiothreitol (DTT) in place of coenzyme A, albeit 300-fold less efficiently (Table 3).

Table 3. Thiol Specificity of Wild-Type BphJ in the Dehydrogenase Reaction[a]

thiol	$K_{m,app}$ (μM)	$k_{cat,app}$ (s^{-1})	$k_{cat}/K_{m,app}$ ($\times 10^4$ M^{-1} s^{-1})
coenzyme A	30.2 ± 2.7	13.9 ± 0.4	46 ± 4
DTT	6609 ± 525	10.1 ± 0.3	0.15 ± 0.01
cysteine	NA	NA	NA
glutathione	NA	NA	NA

[a]Assays were performed at 25 °C and contained 5 μg of BphJ variants, 1 mM $MnCl_2$, 5K_m acetaldehyde, and 400 μM NAD^+ with concentrations of thiols varying between 0.1K_m and 5K_m in 100 mM HEPES buffer (pH 8.0). NA means not available.

This difference was the direct result of the higher K_m value for DTT relative to that for coenzyme A. Free cysteine and

dx.doi.org/10.1021/bi300407y | Biochemistry 2012, 51, 4558–4567

glutathione were not observed to act in lieu of coenzyme A in the dehydrogenase reaction. BphJ had no detectable activity (<0.0001 s^{-1}) in the absence of coenzyme A and DTT, indicating that water cannot replace the thiols in the deacylation step under standard assay conditions.

The wild-type enzyme exhibited a dissociation constant (K_d) for NAD^+ of 1.8 ± 0.2 μM (Table 4). The K_d for NAD^+ in the N170D variant increased by only 1.7-fold, while substitution with alanine, which is not capable of direct hydrogen bonding to the C2 and C3 hydroxyls of the nicotinamide ribose, led to an increase in K_d of ∼4-fold. In comparison, substitution of the adjacent residue, Ile-171 (located ∼7 Å from the nicotinamide moiety of NAD^+), with alanine led to a 20-fold increase in K_d for NAD^+. The K_m values for all variants were determined to ensure all cofactors were present under saturating conditions (Tables S2 and S3 of the Supporting Information). It was observed that the I171A variant had ∼15-fold higher K_m values (>400 μM) for NAD^+ relative to that of the wild-type enzyme.

Table 4. Dissociation Constants of NAD^+ for the Wild Type and Variants[a]

enzyme	K_d (μM)
WT	1.8 ± 0.2
N170A	8 ± 1
N170D	3.2 ± 0.4
I171A	36 ± 4
C131A	48 ± 6
C131S	43 ± 7

[a]Dissociation constants were determined by monitoring tryptophan fluorescence quenching upon NAD^+ binding (excitation wavelength of 295 nm and emission wavelength of 330 nm). The titrations were conducted in 500 μL of 20 mM HEPES (pH 8.5) at 25 °C with 100 μg of enzyme, with stepwise addition of NAD^+ aliquots. Mixtures containing no NAD^+ were used as a control.

Acetaldehyde Substrate Channeling. The acetaldehyde channeling efficiency in N170A was observed to be 83 ± 2% (Table 5). Similar channeling efficiencies were observed in N170D. The I195A variant exhibited a channeling efficiency similar to those of other variants tested (∼80%), while I195W displayed a more dramatic decrease in acetaldehyde channeling efficiency (59 ± 1%). Substitution of Ile-171 with either alanine or phenylalanine resulted in a 20−30% decrease in channeling efficiency.

Table 5. Acetaldehyde Channeling Efficiencies in BphI-BphJ Variant Complexes[a]

BphJ	channeling efficiency (%)
WT	95 ± 5
N170A	83 ± 2
N170D	83 ± 2
I171A	84 ± 3
I171F	77 ± 6
I195W	59 ± 1
I195A	84 ± 1

[a]Assays contained NAD^+ at 5K_m concentrations, coenzyme A at at least 3K_m concentrations, 1 mM $MnCl_2$, 5 μg of enzyme complex, and 20 units of aldehyde dehydrogenase (ALDH), which converts acetaldehyde to acetic acids. Reactions were quenched after 5 min with 24 μL of 3 N HCl. Acetyl-CoA produced was detected at 254 nm by HPLC.

Allosteric Communication. In the wild-type aldolase−dehydrogenase complex, the aldol cleavage activity of BphI is activated in the presence of the BphJ cofactor, NADH, by ∼5-fold.[19,20] When both enzymes are undergoing turnover, this level of activation is increased to 16-fold over that of the nonactivated aldolase. The level of allosteric activation of the aldol cleavage reaction in the presence of the NADH in I171A, N170A, and N170D was observed to be less than 2-fold (Table 6). When BphJ is undergoing turnover, BphI activities when in complex with the I171A, N170A, and N170D BphJ variants were 2.45, 0.91, and 0.54 s^{-1}, respectively, representing 3.6-, 2.1-, and 2.5-fold increases in the catalytic rate, respectively. Thus, these variants result in a significant reduction in the level of activation of the aldol cleavage reaction by BphI.

Table 6. Effects of NADH on Steady-State Kinetic Parameters for the Aldol Cleavage of HOPA by BphI[a]

BphJ in the complex		$K_{m,app}$ (μM)	$k_{cat,app}$ ($\times 10^{-2}$ s^{-1})	x-fold activation by NADH[b]
WT	− NADH	158 ± 20	79 ± 6	−
	+ NADH	89 ± 8	407 ± 7	5.1 ± 0.4
I171A	− NADH	152 ± 22	68 ± 3	−
	+ NADH	28 ± 5	96 ± 3	1.4 ± 0.1
N170A	− NADH	110 ± 12	44 ± 1	−
	+ NADH	32 ± 5	51 ± 2	1.2 ± 0.1
N170D	− NADH	192 ± 18	22 ± 1	−
	+ NADH	34 ± 5	36 ± 1	1.6 ± 0.1

[a]Assays contained 1 mM $MnCl_2$ and HOPA concentrations that varied from 0.1K_m to 10K_m in 100 mM HEPES buffer (pH 8.0). [b]Ratio of k_{cat} (s^{-1}) of BphI in the presence of NADH (final concentration of 0.4 mM) and in the absence of NADH (no NADH added to the assays).

DISCUSSION

BphJ is a nonphosphorylating acylating aldehyde dehydrogenase that catalyzes the acylation of acetaldehyde to acetyl-CoA in the presence of NAD^+ and CoASH. Interestingly, BphJ and related enzymes from bacterial aromatic hydrocarbon degradation pathways share no structural or sequence identity with the only other acylating aldehyde dehydrogenase with known structure, methylmalonate-semialdehyde dehydrogenase from *B. subtilis*.[18] Instead, BphJ and orthologs are evolutionarily related, on the basis of structure, to phosphorylating ALDHs, aspartate-β-semialdehyde dehydrogenase (ASADH) and glyceraldehyde-3-phosphate dehydrogenase (GAPDH).

Replacement of Cys-131 in BphJ with alanine and serine led to the abolishment of BphJ activity. Cys-132 in DmpF is in the same relative position with respect to catalytic thiols of ASADH and GAPDH. Unlike structurally similar GAPDH and ASADH, BphJ and its homologues lack an invariant histidine located proximal to the cysteine residue that is proposed to activate the catalytic thiol[38−41] or to stabilize a tetrahedral transition state.[15,42] It was previously proposed that the conserved Asp-209 in DmpF (Asp-208 in BphJ) is required to activate the Cys-132 via a bound water molecule observed in the apo structure.[23,36] However, the BphJ D208A variant was not significantly affected either in terms of its steady-state kinetic parameters or in its pH profile, discounting the involvement of this residue in the catalytic mechanism. A single ionizable group was observed in both free and bound forms of the BphJ. However, in the substrate-bound form, the pK_a of this group was ∼0.5 pH unit lower than that of the free enzyme. A similar

dx.doi.org/10.1021/bi300407y | Biochemistry 2012, 51, 4558−4567

shift was observed in methylmalonate-semialdehyde dehydrogenase whereby the enzyme exhibits pK_a values of 8.7 and 8.0 for the free enzyme and the enzyme−substrate−NAD^+ binary complex, respectively.[18,43] These pK_a values were assigned to the catalytic cysteine with augmentation of the pK_a in the binary complex attributed to NAD^+. Cofactor binding has also been implicated in thiol activation in nonphosphorylating GAPDH where binding of $NADP^+$ and NAD^+ increases the reactivity of the catalytic thiol.[44,45] Structurally, the nicotinamide ring is ∼4 Å from the thiol group of Cys-132 in the NAD^+-bound structure of DmpF, which supports its role in activating the catalytic thiol.

Replacement of Ile-195 with alanine (I195A) increased the size of the active site, allowing for the accommodation of longer and bulkier aldehydes and hence increasing the specificity constants for these substrates. The specificity constant for acetaldehyde was lowered in this variant, possibly because of the loss of specific interactions between the enzyme and the shorter substrate leading to nonproductive binding. Conversely, incorporation of bulky aromatic residues at position 195 in I195F and I195W perturbed the binding of longer alkyl chain aldehydes. These data suggest that the aldehyde side chain extends toward Ile-195.

Invariant residues Arg-245 and Glu-220 in ASADH from *S. pneumoniae* (PDB entry 2GZ3) are spatially equivalent to Met-198 and Ile-196 in DmpF, respectively.[46,47] Kinetic studies[48] and structures of native enzyme complexes containing a hemithioacetal intermediate[39,47,49] or the inactivator *S*-methyl-L-cysteine sulfoxide[50] have further established that Arg-245 forms bidenate interactions with the α-carboxyl group of the substrate L-aspartate-β-semialdehyde. The role of Glu-220 in ASADHs has not been definitively established,[46] but the side chain carboxyl group may interact with the α-amino group of L-aspartate-β-semialdehyde.[47,49] Residues Arg-231 and Arg-195 in glyceraldehyde-3-phosphate dehydrogenase (GAPDH) of *B. stearothermophilus* (PDB entry 1NQA) are similar in position to Ile-196 in DmpF and Ile-172, respectively. These residues have been implicated in binding the phosphate group of the substrate.[51] Thus, divergent substrate specificities of these evolutionarily related enzymes may be governed by the side chains of the two residues at the back of the active sites of these enzymes (Figure 1C).

Replacement of Ile-171 with alanine led to a 20-fold increase in the NAD^+ dissociation constant for BphJ. In DmpG, the equivalent residue Ile-172, is located on the N-terminus on an α-helix and forms hydrophobic interactions with Ile-196 and Met-198 on an opposing β-sheet. It is envisaged that shortening the side chain in the BphJ I171A variant may disrupt this interaction, thereby altering the Cα backbone and affecting the tertiary structure of the NAD^+-binding domain (Figure 3A). Dissociation constants for the Asn-170 variants of BphJ were also increased, but by <10-fold, indicating that although Asn-170 interacts with NAD^+, it is not critical for cofactor binding. Thus, when Asn-170 is replaced with aspartate or shortened to alanine, hydrogen bonding with NAD^+ can still occur between the carboylate oxygen and ribosyl hydroxyls in N170D, or space may be created for water molecules to interact with NAD^+ in N170A. Indeed, in the structurally similar GAPDH and ASADH, NAD^+ binds in a position similar to that of DmpF (Figure 1C), but ordered water molecules form hydrogen bond interactions with the hydroxyls of the ribose of NAD^+ instead.

Substrate Channeling and Allostery. By inference from the DmpF structure[23] and previous channel identification using MOLE,[19] Ile-171, Ile-195, and Leu-197 in BphJ form the exit of the substrate channel connecting the active sites of the aldolase and dehydrogenase. This was confirmed by reduced aldehyde channeling efficiencies when Ile-195 was replaced with bulky residues phenylalanine and tryptophan. A BphJ I195F variant was previously demonstrated to have a channeling efficiency of 80 ± 1%,[19] while I195W exhibited a channeling efficiency of 59 ± 1%. Aldehyde channeling in the BphI-BphJ system is still efficient (83 ± 2%) when Asn-170 was replaced with alanine, which cannot form hydrogen bond interactions with the ribosyl hydroxyls of the nicotinamide moiety of NAD^+. Therefore, the previous proposal,[23] that substrate channeling is dependent on hydrogen bonding interaction between the side chain of Asn-171 (Asn-170 in BphJ) and NAD^+, which alters the Cα backbone and rotameric configuration of Ile-172, Ile-196, and Met-198 to allow the exit of the channeled aldehyde, is not supported by the experimental evidence. In comparison, Tyr-290 in BphI partially blocks the entrance of the aldehyde channel. Previous replacement of Tyr-290 compromised channeling efficiency (up to 85% reduction in channeling efficiency). Therefore, Tyr-290 in the aldolase appears to be the important gating residue for aldehyde channeling in BphI-BphJ.[19]

Interestingly, Asn-170 and Ile-171 appear to be important in mediating allosteric activation of the aldol cleavage reaction of BphI upon NAD^+ binding in BphJ. Replacement of these residues led to attenuation of BphI activation. This allostery likely ensures that aldehydes released to the solvent in the absence of cofactors are kept to a minimum because the aldol cleavage reaction always occurs in the presence of 4-hydroxy-2-oxoacids. The equivalent Asn-171 and Ile-172 are located in the α7 and α8 secondary structures of DmpF that interact with the α5 secondary structure of the HMGL-like domain in the aldolase, DmpG. It is possible that the allosteric activation is mediated through these intersubunit contacts. However, the precise molecular mechanism of this activation is currently unclear because no obvious structural changes in the aldolase can be observed between the crystal structures of the apo and NAD^+-bound forms of the DmpF-DmpG complex.

CONCLUSION

In summary, BphJ utilizes Cys-131 as the catalytic thiol; however, this thiol is not activated by Asp-208 as previously proposed.[23,36] Ile-195 is involved in substrate binding, and residues in equivalent positions in phosphorylating ALDHs also appear to interact with their respective substrates. Interaction of Asn-170 with the nicotinamide cofactor does not appear to be important for substrate channeling. However, Asn-170 and Ile-171 are important for allosteric activation of BphI. The results presented herein complement our previous work and shed further light on the mechanism of substrate channeling in this enzyme complex.[19−22,32,52]

ASSOCIATED CONTENT

Supporting Information

Circular dichroism spectra of wild-type BphJ and its C131A and C131S variants (Figure S1), primers used in polymerase chain reaction site-directed mutagenesis (Table S1), steady-state kinetic parameters of BphJ variants (Table S2), and steady-state kinetic parameters of BphJ cofactors (Table S3). This material is available free of charge via the Internet at http://pubs.acs.org.

AUTHOR INFORMATION

Corresponding Author

*Department of Molecular and Cellular Biology, University of Guelph, Guelph, Ontario, Canada N1G 2W1. E-mail: sseah@uoguelph.ca. Phone: (519) 824-4120, ext. 56750. Fax: (519) 837-1802.

Author Contributions

P.B. and J.C. contributed equally to this work.

Funding

This research is supported by the National Science and Engineering Research Council of Canada (NSERC), Grant 238284 (to S.Y.K.S.). P.B. is a recipient of a postgraduate research scholarship from NSERC.

Notes

The authors declare no competing financial interest.

ABBREVIATIONS

ADH, alcohol dehydrogenase; ALDH, aldehyde dehydrogenase; ASADH, aspartate-semialdehyde dehydrogenase; EDTA, ethylenedinitrilotetraacetic acid; GAPDH, glyceraldehyde-3-phosphate dehydrogenase; HEPES, 4-(2-hydroxyethyl)-1-piperazinepropanesulfonic acid; HOPA, 4-hydroxy-2-oxopentanoate; IPTG, isopropyl β-D-thiogalactopyranoside; LDH, L-lactate dehydrogenase; MES, 2-(*N*-morpholino)ethanesulfonic acid.

REFERENCES

(1) Segal, H. L., and Boyer, P. D. (1953) The role of sulfhydryl groups in the activity of D-glyceraldehyde 3-phosphate dehydrogenase. *J. Biol. Chem. 204*, 265−281.

(2) Racker, E., and Krimsky, I. (1952) The mechanism of oxidation of aldehydes by glyceraldehyde-3-phosphate dehydrogenase. *J. Biol. Chem. 198*, 731−743.

(3) Feldman, R. I., and Weiner, H. (1972) Horse liver aldehyde dehydrogenase. II. Kinetics and mechanistic implications of the dehydrogenase and esterase activity. *J. Biol. Chem. 247*, 267−272.

(4) Bradbury, S. L., and Jakoby, W. B. (1971) Ordered binding of substrates to yeast aldehyde dehydrogenase. *J. Biol. Chem. 246*, 1834−1840.

(5) MacGibbon, A. K., Blackwell, L. F., and Buckley, P. D. (1977) Pre-steady-state kinetic studies on cytoplasmic sheep liver aldehyde dehydrogenase. *Biochem. J. 167*, 469−477.

(6) Vallari, R. C., and Pietruszko, R. (1981) Kinetic mechanism of the human cytoplasmic aldehyde dehydrogenase E1. *Arch. Biochem. Biophys. 212*, 9−19.

(7) Marchal, S., Rahuel-Clermont, S., and Branlant, G. (2000) Role of glutamate-268 in the catalytic mechanism of nonphosphorylating glyceraldehyde-3-phosphate dehydrogenase from *Streptococcus mutans*. *Biochemistry 39*, 3327−3335.

(8) Shone, C. C., and Fromm, H. J. (1981) Steady-state and pre-steady-state kinetics of coenzyme A linked aldehyde dehydrogenase from *Escherichia coli*. *Biochemistry 20*, 7494−7501.

(9) Sohling, B., and Gottschalk, G. (1993) Purification and characterization of a coenzyme-A-dependent succinate-semialdehyde dehydrogenase from *Clostridium kluyveri*. *Eur. J. Biochem. 212*, 121−127.

(10) Yan, R. T., and Chen, J. S. (1990) Coenzyme A-acylating aldehyde dehydrogenase from *Clostridium beijerinckii* NRRL B592. *Appl. Environ. Microbiol. 56*, 2591−2599.

(11) Farres, J., Wang, T. T., Cunningham, S. J., and Weiner, H. (1995) Investigation of the active site cysteine residue of rat liver mitochondrial aldehyde dehydrogenase by site-directed mutagenesis. *Biochemistry 34*, 2592−2598.

(12) Wang, X., and Weiner, H. (1995) Involvement of glutamate 268 in the active site of human liver mitochondrial (class 2) aldehyde dehydrogenase as probed by site-directed mutagenesis. *Biochemistry 34*, 237−243.

(13) Vedadi, M., and Meighen, E. (1997) Critical glutamic acid residues affecting the mechanism and nucleotide specificity of *Vibrio harveyi* aldehyde dehydrogenase. *Eur. J. Biochem. 246*, 698−704.

(14) Cobessi, D., Tete-Favier, F., Marchal, S., Branlant, G., and Aubry, A. (2000) Structural and biochemical investigations of the catalytic mechanism of an NADP-dependent aldehyde dehydrogenase from *Streptococcus mutans*. *J. Mol. Biol. 300*, 141−152.

(15) Soukri, A., Mougin, A., Corbier, C., Wonacott, A., Branlant, C., and Branlant, G. (1989) Role of the histidine 176 residue in glyceraldehyde-3-phosphate dehydrogenase as probed by site-directed mutagenesis. *Biochemistry 28*, 2586−2592.

(16) D'Ambrosio, K., Pailot, A., Talfournier, F., Didierjean, C., Benedetti, E., Aubry, A., Branlant, G., and Corbier, C. (2006) The first crystal structure of a thioacylenzyme intermediate in the ALDH family: New coenzyme conformation and relevance to catalysis. *Biochemistry 45*, 2978−2986.

(17) Talfournier, F., Pailot, A., Stines-Chaumeil, C., and Branlant, G. (2009) Stabilization and conformational isomerization of the cofactor during the catalysis in hydrolytic ALDHs. *Chem.-Biol. Interact. 178*, 79−83.

(18) Talfournier, F., Stines-Chaumeil, C., and Branlant, G. (2011) Methylmalonate-semialdehyde dehydrogenase from *Bacillus subtilis*: Substrate specificity and coenzyme A binding. *J. Biol. Chem. 286*, 21971−21981.

(19) Carere, J., Baker, P., and Seah, S. Y. (2011) Investigating the Molecular Determinants for Substrate Channeling in BphI-BphJ, an Aldolase-Dehydrogenase Complex from the Polychlorinated Biphenyls Degradation Pathway. *Biochemistry 50*, 8407−8416.

(20) Baker, P., Pan, D., Carere, J., Rossi, A., Wang, W., and Seah, S. Y. (2009) Characterization of an aldolase-dehydrogenase complex that exhibits substrate channeling in the polychlorinated biphenyls degradation pathway. *Biochemistry 48*, 6551−6558.

(21) Wang, W., Baker, P., and Seah, S. Y. (2010) Comparison of two metal-dependent pyruvate aldolases related by convergent evolution: Substrate specificity, kinetic mechanism, and substrate channeling. *Biochemistry 49*, 3774−3782.

(22) Baker, P., Carere, J., and Seah, S. Y. (2011) Probing the Molecular Basis of Substrate Specificity, Stereospecificity, and Catalysis in the Class II Pyruvate Aldolase, BphI. *Biochemistry 50*, 3559−3569.

(23) Manjasetty, B. A., Powlowski, J., and Vrielink, A. (2003) Crystal structure of a bifunctional aldolase-dehydrogenase: Sequestering a reactive and volatile intermediate. *Proc. Natl. Acad. Sci. U.S.A. 100*, 6992−6997.

(24) Dubourg, H., Stines-Chaumeil, C., Didierjean, C., Talfournier, F., Rahuel-Clermont, S., Branlant, G., and Aubry, A. (2004) Expression, purification, crystallization and preliminary X-ray diffraction data of methylmalonate-semialdehyde dehydrogenase from *Bacillus subtilis*. *Acta Crystallogr. D60*, 1435−1437.

(25) Lei, Y., Pawelek, P. D., and Powlowski, J. (2008) A shared binding site for NAD^+ and coenzyme A in an acetaldehyde dehydrogenase involved in bacterial degradation of aromatic compounds. *Biochemistry 47*, 6870−6882.

(26) Ricagno, S., Jonsson, S., Richards, N., and Lindqvist, Y. (2003) Crystallization and preliminary crystallographic analysis of formyl-CoA tranferase from *Oxalobacter formigenes*. *Acta Crystallogr. D59*, 1276−1277.

(27) Ricagno, S., Jonsson, S., Richards, N., and Lindqvist, Y. (2003) Formyl-CoA transferase encloses the CoA binding site at the interface of an interlocked dimer. *EMBO J. 22*, 3210−3219.

(28) Wolodko, W. T., Fraser, M. E., James, M. N., and Bridger, W. A. (1994) The crystal structure of succinyl-CoA synthetase from *Escherichia coli* at 2.5-Å resolution. *J. Biol. Chem. 269*, 10883−10890.

(29) Liu, H., and Naismith, J. H. (2008) An efficient one-step site-directed deletion, insertion, single and multiple-site plasmid mutagenesis protocol. *BMC Biotechnol. 8*, 91.

(30) Bradford, M. M. (1976) A rapid and sensitive method for the quantitation of microgram quantities of protein utilizing the principle of protein-dye binding. *Anal. Biochem. 72*, 248−254.
(31) Cornish-Bowden, A. (1995) *Analysis of enzyme kinetic data*, Oxford University Press, New York.
(32) Baker, P., Hillis, C., Carere, J., and Seah, S. Y. (2012) Protein-protein interactions and substrate channeling in orthologous and chimeric aldolase-dehydrogenase complexes. *Biochemistry 51*, 1942−1952.
(33) Holm, L., and Rosenstrom, P. (2010) Dali server: Conservation mapping in 3D. *Nucleic Acids Res. 38*, W545−W549.
(34) Viola, R. E., Liu, X., Ohren, J. F., and Faehnle, C. R. (2008) The structure of a redundant enzyme: A second isoform of aspartate β-semialdehyde dehydrogenase in *Vibrio cholerae*. *Acta Crystallogr. D64*, 321−330.
(35) Charron, C., Talfournier, F., Isupov, M. N., Littlechild, J. A., Branlant, G., Vitoux, B., and Aubry, A. (2000) The crystal structure of D-glyceraldehyde-3-phosphate dehydrogenase from the hyperthermophilic archaeon *Methanothermus fervidus* in the presence of $NADP^+$ at 2.1 Å resolution. *J. Mol. Biol. 297*, 481−500.
(36) Smith, N. E., Vrielink, A., Attwood, P. V., and Corry, B. (2012) Biological Channeling of a Reactive Intermediate in the Bifunctional Enzyme DmpFG. *Biophys. J. 102*, 868−877.
(37) Kleywegt, G. J., Harris, M. R., Zou, J. Y., Taylor, T. C., Wahlby, A., and Jones, T. A. (2004) The Uppsala Electron-Density Server. *Acta Crystallogr. D60*, 2240−2249.
(38) Moras, D., Olsen, K. W., Sabesan, M. N., Buehner, M., Ford, G. C., and Rossmann, M. G. (1975) Studies of asymmetry in the three-dimensional structure of lobster D-glyceraldehyde-3-phosphate dehydrogenase. *J. Biol. Chem. 250*, 9137−9162.
(39) Blanco, J., Moore, R. A., and Viola, R. E. (2003) Capture of an intermediate in the catalytic cycle of L-aspartate-β-semialdehyde dehydrogenase. *Proc. Natl. Acad. Sci. U.S.A. 100*, 12613−12617.
(40) Blanco, J., Moore, R. A., Faehnle, C. R., and Viola, R. E. (2004) Critical catalytic functional groups in the mechanism of aspartate-β-semialdehyde dehydrogenase. *Acta Crystallogr. D60*, 1808−1815.
(41) Zhang, L., Ahvazi, B., Szittner, R., Vrielink, A., and Meighen, E. (2000) A histidine residue in the catalytic mechanism distinguishes *Vibrio harveyi* aldehyde dehydrogenase from other members of the aldehyde dehydrogenase superfamily. *Biochemistry 39*, 14409−14418.
(42) Talfournier, F., Colloc'h, N., Mornon, J. P., and Branlant, G. (1998) Comparative study of the catalytic domain of phosphorylating glyceraldehyde-3-phosphate dehydrogenases from bacteria and archaea via essential cysteine probes and site-directed mutagenesis. *Eur. J. Biochem. 252*, 447−457.
(43) Stines-Chaumeil, C., Talfournier, F., and Branlant, G. (2006) Mechanistic characterization of the MSDH (methylmalonate semialdehyde dehydrogenase) from *Bacillus subtilis*. *Biochem. J. 395*, 107−115.
(44) Marchal, S., Cobessi, D., Rahuel-Clermont, S., Tete-Favier, F., Aubry, A., and Branlant, G. (2001) Chemical mechanism and substrate binding sites of NADP-dependent aldehyde dehydrogenase from *Streptococcus mutans*. *Chem.-Biol. Interact. 130−132*, 15−28.
(45) Harris, J. I., and Waters, M. (1976) *The Enzymes*, 3rd ed., Academic Press, San Diego.
(46) Blanco, J., Moore, R. A., Faehnle, C. R., Coe, D. M., and Viola, R. E. (2004) The role of substrate-binding groups in the mechanism of aspartate-β-semialdehyde dehydrogenase. *Acta Crystallogr. D60*, 1388−1395.
(47) Faehnle, C. R., Ohren, J. F., and Viola, R. E. (2005) A new branch in the family: Structure of aspartate-β-semialdehyde dehydrogenase from *Methanococcus jannaschii*. *J. Mol. Biol. 353*, 1055−1068.
(48) Ouyang, J., and Viola, R. E. (1995) Use of structural comparisons to select mutagenic targets in aspartate-β-semialdehyde dehydrogenase. *Biochemistry 34*, 6394−6399.
(49) Faehnle, C. R., Le Coq, J., Liu, X., and Viola, R. E. (2006) Examination of key intermediates in the catalytic cycle of aspartate-β-semialdehyde dehydrogenase from a Gram-positive infectious bacteria. *J. Biol. Chem. 281*, 31031−31040.
(50) Blanco, J., Moore, R. A., Kabaleeswaran, V., and Viola, R. E. (2003) A structural basis for the mechanism of aspartate-β-semialdehyde dehydrogenase from *Vibrio cholerae*. *Protein Sci. 12*, 27−33.
(51) Skarzynski, T., Moody, P. C., and Wonacott, A. J. (1987) Structure of holo-glyceraldehyde-3-phosphate dehydrogenase from *Bacillus stearothermophilus* at 1.8 Å resolution. *J. Mol. Biol. 193*, 171−187.
(52) Baker, P., and Seah, S. Y. (2012) Rational design of stereoselectivity in the class II pyruvate aldolase BphI. *J. Am. Chem. Soc. 134*, 507−513.